Published OnlineFirst March 3, 2009; DOI: 10.1158/1535-7163.MCT-08-0570

MEK/ERK inhibitor U0126 affects *in vitro* and *in vivo* growth of embryonal rhabdomyosarcoma

Francesco Marampon,[1,3] Gianluca Bossi,[2] Carmela Ciccarelli,[1] Agnese Di Rocco,[1] Ada Sacchi,[2] Richard G. Pestell,[3] and Bianca M. Zani[1]

[1]Department of Experimental Medicine, University of L'Aquila, L'Aquila, Italy; [2]Department of Experimental Oncology, Regina Elena Cancer Institute, Rome, Italy; and [3]Department of Cancer Biology and Medical Oncology, Kimmel Cancer Center, Thomas Jefferson University, Philadelphia, Pennsylvania

Abstract

We reported previously that the disruption of c-Myc through mitogen-activated protein kinase kinase (MEK)/extracellular signal-regulated kinase (ERK) inhibition blocks the expression of the transformed phenotype in the embryonal rhabdomyosarcoma (ERMS) cell line (RD), thereby inducing myogenic differentiation *in vitro*. In this article, we investigate whether MEK/ERK inhibition, by the MEK/ERK inhibitor U0126, affects c-Myc protein level and growth of RMS tumor in an *in vivo* xenograft model. U0126 significantly reduced RMS tumor growth in RD cell line-xenotransplanted mice. Immunobiochemical and immunohistochemical analysis showed (*a*) phospho-active ERK levels were reduced by U0126 therapy and unaltered in normal tissues, (*b*) phospho-Myc and c-Myc was reduced commensurate with phospho-ERK inhibition, and (*c*) reduction in Ki-67 and endothelial (CD31) marker expression. These results indicate that MEK/ERK inhibition affects growth and angiogenic signals in tumor. The RD-M1 cultured xenograft tumor-derived cell line and the ERMS cell line TE671 responded to U0126 by arresting growth, down-regulating c-Myc, and initiating myogenesis. All these results suggest a tight correlation of MEK/ERK inhibition with c-Myc down-regulation and arrest of tumor growth. Thus, MEK inhibitors may be investigated for a signal transduction-based targeting of the c-Myc as a therapeutic strategy in ERMS. [Mol Cancer Ther 2009; 8(3):543–51]

Received 6/19/08; revised 11/26/08; accepted 1/8/09; published OnlineFirst 3/3/09.

Grant support: University of L'Aquila.

The costs of publication of this article were defrayed in part by the payment of page charges. This article must therefore be hereby marked *advertisement* in accordance with 18 U.S.C. Section 1734 solely to indicate this fact.

Requests for reprints: Bianca M. Zani, Department of Experimental Medicine, University of L'Aquila, Via Vetoio Coppito II, 67100 L'Aquila, Italy. Phone: 39-0862-433514; Fax: 39-0862-433523. E-mail: biancamaria.zani@univaq.it

doi:10.1158/1535-7163.MCT-08-0570

Introduction

Malignant tumors of skeletal muscle rhabdomyosarcomas (RMS) are the most common soft-tissue sarcoma in childhood. RMS is thought to derive from cells along the skeletal muscle cell axis (1). The embryonal RMS (ERMS) and the alveolar subtypes (ARMS; refs. 2, 3) harbor mutation of the p53, N-Ras, or K-Ras genes and deregulation of imprinted genes in chromosome region 11p15.5 (2, 4–8).

The Ras/Raf/mitogen-activated protein kinase kinase (MEK)/extracellular signal-regulated kinase (ERK) cascade regulates proliferation, differentiation, survival, motility, and tissue formation (9–12). Ras mutation activating MEKs and ERKs occurs in a relatively large number of human tumors (13–15). Raf or Ras mutations predict sensitivity to MEK inhibitors and the pharmacologic MEK inhibition counteracts growth of Raf or Ras mutant xenografts (16) and are currently being investigated as anticancer drugs in combined therapies (14). U0126, the MEK/ERK inhibitor, prevents activation of MEK1/2 and blocks activated MEK1/2 (17). c-Myc is targeted by ERKs that induce c-Myc stability, whereas GSK-3β induces c-Myc degradation (18, 19). This regulation of c-Myc suggests that constitutive Ras activation could be responsible of chronic MEK/ERK activation and phosphatidyinositol 3-kinase/AKT-mediated GSK-3β inactivation leading to c-Myc aberrant accumulation (20).

c-Myc, N-Myc, and MYCL1 play a role in human cancer (21). c-Myc transformation is dependent on dimerization with the HLH-LZ protein Max; Myc/Max heterodimer drives Myc to E-boxes of oncogenic target genes (22). In conditional transgenic models on Myc inactivation, tumors can regress (23, 24). Several strategies have been designed to disrupt c-Myc (25). No clear data are yet available on amplification of specific Myc member in ERMS; by contrast, N-Myc amplification has been detected in alveolar RMS (26).

We showed previously in ERMS (RD) *in vitro* that the RD phenotype could be reversed *in vitro* by disrupting c-Myc through MEK/ERK inhibition (27).

We therefore investigated whether MEK/ERK inhibition, by the MEK/ERK inhibitor U0126, affects growth of RMS tumor and c-Myc protein level in an *in vivo* model of xenograft. Herein, U0126 treatment of RMS-xenografted nude mice reduced tumor growth and phospho-ERK and c-Myc expression. This responsiveness to U0126 occurred in another ERMS cell line, TE671, and in a more tumorigenic xenografted-derived cell line (RD-M1) *in vitro*, thereby corroborating the idea that MEK inhibition may offer a new means of developing novel anticancer strategies versus ERMS types.

Materials and Methods

Cell Cultures and Treatments

The human ERMS (American Type Culture Collection) RD cell lines and TE671 (HTL97021; Interlab Cell Line

Published OnlineFirst March 3, 2009; DOI: 10.1158/1535-7163.MCT-08-0570

Collection) were cultured in DMEM supplemented with glutamine, pyruvate, gentamycin (Life Technologies), and 10% heat-inactivated fetal bovine serum (JRH Biosciences). Treatment with 10 μmol/L kinase inhibitor U0126 (1,4-diamino-2,3-dicyano-1,4-bis[2-aminophenylthio]butadiene; Promega) was done for the times shown in the figures and started 1 day after plating. Primary human SkMC cells (PromoCell) were cultured according to the manufacturer's instructions in growth medium for 4 days. The neuroblastoma cell line (SH-Sy5y) was grown as described (28).

Xenograft and U0126 Treatment

To determine the most suitable concentration of RD cells to develop tumors as a xenograft model, exponentially growing RD cells were detached by trypsin-EDTA, washed twice in PBS, and resuspended in saline solution at two cell densities (1×10^6 and 1×10^7 per 200 μL). Xenotransplants were done in 45-day-old female athymic nude mice (*CD1*; Charles River) by s.c. injection in the intrascapular area using a 21-gauge syringe. Mice were kept under sterile conditions, receiving sterile nutrition and water. All the procedures involving animals and their care were conducted in conformity with the institutional guidelines. Tumor size was measured by caliper according to the following formula: volume = $(\text{width})^2 \times \text{length} / 2$. An endpoint of 2.0 to 2.5 cm^3 was adopted for tumor size.

U0126 treatment was done in mice xenotransplanted with 1×10^7 cells and started when tumors reached a volume of 0.2 to 0.3 cm^3. U0126 solution was prepared in DMSO as a stock solution of 10 μmol/L, and the amount of drug to be injected into a set of mice was diluted with carrier solution (40% DMSO in physiologic solution). Two hundred microliters containing either 25 or 50 μmol/kg was injected i.p. into each mouse. Control xenotransplants were treated with 200 μL/mouse carrier solution.

Statistical Analysis

Student's t test was used for the comparison of groups; data were considered significant when $P < 0.05$.

Derivation of RD-M1 Cell Line from Xenografted Tumor, Growth Curve, and Fluorescence-Activated Cell Sorting Analysis

Tumor from untreated mouse was excised and washed in complete medium and physiologic solution, minced with scissors, collected, and resuspended in trypsin-EDTA. Trypsin treatment was repeated three times to dissociate the cells from the tumor mass. The cells obtained were plated and grown until confluence in complete medium as described above for the RD cell line. Three subsequent passages were sufficient to remove contaminating cells from vessels and connective tissue. The purified cell line, RD-M1, was grown in culture and treated as described above for the RD cell line. The growth curve was obtained by growing cells in complete medium in the presence and in the absence of 10 μmol/L U0126 for different time intervals. Cells were harvested, washed, resuspended in PBS and counted in a hemocytometer chamber. Fluorescence-activated cell sorting (FACS) analysis was done as described in our previous article (29). RD-M1 cells line were also used in a xenograft experiment following the aforementioned protocol.

Immunoblot Analysis

Western blotting was conducted as described previously (30, 31). Briefly, cells from cultures were lysed in 2% SDS containing phosphatase and protease inhibitors (Roche) sonicated for 30 s. Proteins of whole-cell lysates were assessed using the Lowry method (32), and equal amounts were separated on SDS-PAGE. Both tumors and normal tissues were crushed in nitrogen, and the powder was collected and resuspended in 2% SDS containing phosphatase and protease inhibitors, sonicated for 30 s, and clarified by centrifugation. Aliquots of tissue extracts were used for total protein evaluation. SDS-PAGE analysis was done as for cultured cells. The proteins were transferred to a nitrocellulose membrane (Schleicher & Schuell, Bioscience) by electroblotting. The total protein level balance was confirmed by staining the membranes with Ponceau S (Sigma).

Immunoblottings were done as described previously (33, 34) with the following antibodies: anti-c-Myc (N-262), anti-c-Myc clone 9E10, anti-N-Myc (C-19), anti-phospho-c-Myc (Thr^{58}/Ser^{62}), anti-phospho-ERK1/2 (E-4), anti-ERK2 (C-14), anti-cyclin E (H-12), anti-cyclin A (H-432), anti-cyclin B1 (H-433), CDK2 (M-2), and α-tubulin (B-7; all from Santa Cruz Biotechnology) and anti-myosin heavy chain (MHC; MF20; gift from D. Fichman). The anti-c-Myc clone 9E10, known not to recognize viral Myc, was used to exclude the expression of v-Myc due to retroviral genomic sequence insertion (Supplementary Fig. S1).[4] Peroxidase-conjugate anti-mouse or anti-rabbit IgG (Amersham GE Healthcare or Santa Cruz Biotechnology) was used for enhanced chemiluminescence detection. Densitometry was done by measuring the pixel density of bands and each value was normalized for α-tubulin; control untreated samples were arbitrarily set at 1.

Histochemistry and Immunofluorescence of Cryosections

Cryosections (10 μm), fixed in PBS 4% paraformaldehyde, and washed before nonspecific binding sites were blocked with 5% bovine serum albumin or goat anti-serum in PBS for 1 h at room temperature. Slides were then incubated overnight at 4°C with the appropriate antibody dilution. After rinsing with PBS, the slides were incubated with 1:1,000 of Cy3 anti-mouse IgG (The Jackson Laboratory) for phospho-ERK, Ki-67 (MIB-1; DakoCytomation), and CD31 (WM-59; Sigma) or Cy3 anti-rabbit IgG for total ERK (The Jackson Laboratory) in the presence of Hoechst, washed, and mounted with Vectashield (Vector Laboratories). Immunofluorescence was visualized using AxioPlan2 ×40 (Zeiss), and for CD31, ×20 objectives with digital images were collected with a Leica DFC350FX camera interfaced with a IM500 Leica software.

After immunofluorescence, the inhibition of nuclear phospho-ERK, c-Myc, and Ki-67 induced by U0126 was estimated by comparing the percentage of positive nuclei (violet in merged images) of U0126-treated tumors versus the percentage of positive nuclei of untreated tumors. Six to eight different cryosections were analyzed from control and treated tumors.

[4] Supplementary material for this article is available at Molecular Cancer Therapeutics Online (http://mct.aacrjournals.org/).

Published OnlineFirst March 3, 2009; DOI: 10.1158/1535-7163.MCT-08-0570

Colony-Forming Assays in Semisolid Agar

Cells were resuspended in 4 mL of 0.33% special Noble agar (Difco) and plated (6 cm plate) in growth medium containing 0.5% soft agar (35). Colonies were photographed 14 days after plating.

Results

c-Myc Rather Than N-Myc Protein and Phospho-ERKs Are Up-Regulated in the RD Cell Line

The Ras/MEK/ERK pathway and c-Myc can cooperate in control of normal and aberrant growth (20), and the Ras/MEK/ERK may increase c-Myc abundance (18). We first analyzed the c-Myc and N-Myc expression in RD cell line. To assess by immunoblotting the Myc protein predominantly expressed in RD cell line, we also used SH-Sy5y cell line, known to preferentially overexpress N-Myc, and human skeletal muscle as a control. c-Myc was detectable in the RD at high levels, whereas N-Myc is slightly detectable. In contrast, N-Myc is the predominant Myc protein in the neuroblastoma cell line SH-Sy5y (Neu), whereas c-Myc is hardly detectable (Fig. 1A). Phospho-ERKs were expressed at a high level in the RD cells and undetectable in SH-Sy5y cells. The c-Myc protein level was severalfold (six times) higher in RD cells compared with human skeletal muscle (Fig. 1B). The concomitant high level of c-Myc and phospho-ERKs suggests that deregulated Ras/MEK/ERK pathway may induce c-Myc in RD cells.

Establishment of RD Xenograft Model in Nude Mice

Xenotransplants were done by s.c. injection in the intrascapular area with either 1.0×10^6 or 1.0×10^7 cells per mouse. Tumor growth was quantified by caliper measurement. Both dilutions induced tumors detectable from the 11th week post-injection (Fig. 2A). For subsequent studies, the higher cell density (1×10^7cells per mouse) was adopted as it induced larger tumors and a higher (100%) tumor uptake from the 13th week post-injection than the lower (1×10^6 cells per mouse) cell density (Fig. 2A and B).

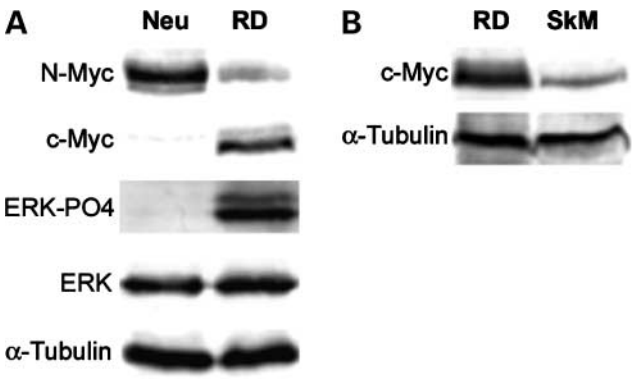

Figure 1. Immunoblotting analysis of N-Myc, c-Myc, and phospho-ERK expression in RMS, neuroblastoma cell lines, and muscle-derived cells. **A,** total cell lysates from RMS (RD) and neuroblastoma-derived cell lines SH-Sy5y (Neu) were analyzed using antibodies specific for N-Myc or c-Myc, phospho-ERK or total ERK, and α-tubulin as loading control. **B,** c-Myc levels in RD and normal human muscle cells (*Sk-M,* skeletal muscle). This analysis was done in three different experiments.

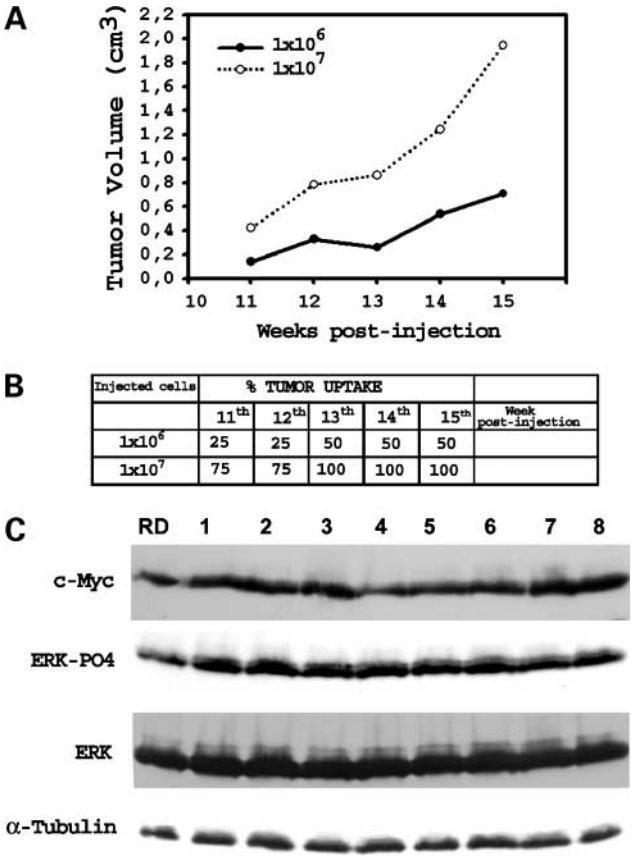

Figure 2. Growth potential of RD cells xenografted in nude mice. **A,** growth curves of tumors from 1×10^6 and 1×10^7 RD cells s.c. inoculated. Tumor size was assessed weekly. **B,** percentage of xenotransplanted mice that develop tumor mass (tumor uptake). **C,** immunoblot of total lysates from cultured RD cell line (RD) and 8 among 10 xenografted tumors (1×10^7 injected cells; *1-8*) using antibodies targeting c-Myc, phospho-ERKs, and ERKs. α-Tubulin was used as loading control.

We investigated c-Myc and phospho-ERK expression levels in the RD xenograft tumor. Results showed that c-Myc and phospho-ERK in the RD xenograft tumors were highly expressed as seen in the *in vitro* cultured RD cells (Fig. 2C).

Effect of U0126 Therapy in RD Xenograft Model

We studied the effects of U0126 in a RD xenograft tumor model in nude mice. Thirty mice were s.c. injected with RD cells (1×10^7 per mouse); after tumors reached a volume of ~ 0.3 cm^3, animals were divided in three groups of 10 mice each. We used 25 and 50 μmol/kg U0126, in accordance with other recent studies (36, 37), administered to the animals through i.p. injections. Animals were injected weekly with either doses of U0126, diluted in 200 μL carrier solution (see Materials and Methods), whereas control animals were injected with 200 μL carrier solution. Treatments were administered for 5 weeks. Tumor sizes were measured weekly throughout the treatment period.

Published OnlineFirst March 3, 2009; DOI: 10.1158/1535-7163.MCT-08-0570

Results obtained with 25 μmol/kg showed that the rate of tumor growth was markedly reduced by U0126 treatment, a 48% reduction in tumor growth being observed at the end of treatment ($P < 0.05$; Fig. 3A). Moreover, in adopted experimental conditions, no substantial differences in reduction of tumor growth were observed between the two dosages tested (25 and 50 μmol/kg; Supplementary Fig. S2).[4]

To detect total ERK and c-Myc levels and their phosphorylation status in tumors, biochemical analyses were done after 4 and 5 weeks of U0126 treatment. Tumors from U0126-treated and control mice (carrier solution) were excised 24 h post-injection, homogenized, and analyzed by immunoblotting. U0126 treatment reduced ERKs phosphorylation (~60%) and reduced total and phospho-c-Myc (~80% and ~70%) compared with tumors from carrier-treated mice (Fig. 3B). Thus, xenografted human RD-derived tumors are sensitive to U0126 after 4 or 5 weeks of treatment (Fig. 3C).

To exclude a generalized effect of the drug, phospho-ERK status was assessed in normal tissues (liver, lung, and brain) from the same animals analyzed in the experiment of Fig. 3B. In normal tissues, neither phospho-ERKs nor total ERKs were inhibited by U0126 (Fig. 3D). The dosages of U0126 tested (25 and 50 μmol/kg) did not produce toxic effects during the 5-week treatment period, with 100% survival.

Immunohistochemical Characteristics of Vehicle- and U0126-Treated Tumors

Results of immunohistochemical examination of tumors in cryosections show that U0126 reduced both nuclear phospho-ERK and c-Myc staining by ~38% and ~60%, respectively (Fig. 4A; Supplementary Fig. S3).[4] Total phospho-ERK immunofluorescence was reduced in U0126-treated tumors as well (Fig. 4A). There was no difference in the total ERK staining between tumors from treated and control mice (Supplementary Fig. S3).[4] In carrier-treated mice, tumors displayed numerous grouped cells with a high nuclear c-Myc positivity, whereas c-Myc positivity was lower and ungrouped in tumors from U0126-treated mice (Fig. 4A).

The marked reduction in the staining of Ki-67 (~74% inhibition; Supplementary Fig. S3)[4] suggests that U0126 treatment inhibited cellular growth. To analyze whether U0126 treatment affects tumor microvessel density, we performed CD31 immunostaining. Results showed that tumors from

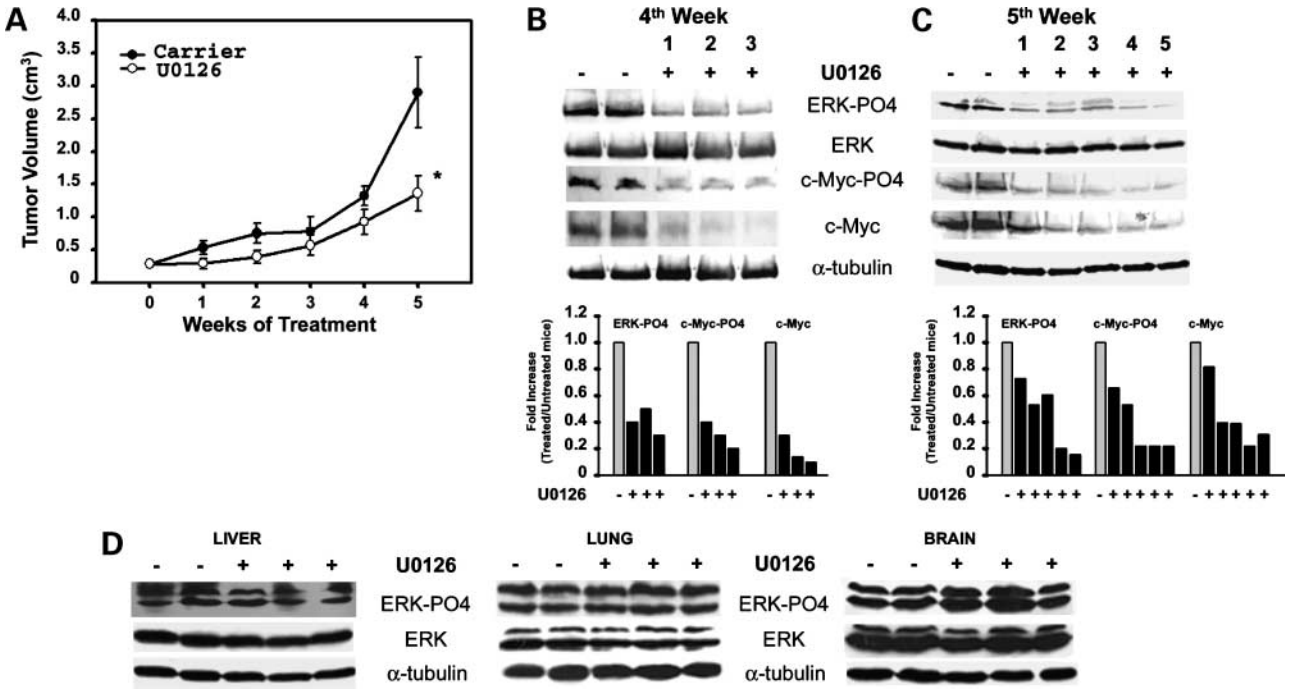

Figure 3. Tumor growth and molecular changes in untreated and U0126-treated mice. **A,** growth curves of xenografted RD cells. U0126 was i.p. inoculated at 25 μmol/kg/mouse (○—○), whereas untreated mice were inoculated with carrier solution (●—●). Mean ± SD of tumor size of mice per group. *, $P < 0.05$ versus control. **B,** effects of U0126 in tumors 24 h post-injection in the 4th week of treatment. *Left,* immunoblot analysis of phospho-ERKs, total ERK, c-Myc, phospho-c-Myc, and α-tubulin as loading control in tumors from treated (+) and untreated (−) mice; *right,* quantification of each sample of the Western blots as a fold increase of the indicated proteins in the U0126-treated mice (*1-3*) over the untreated mice (*C*) arbitrarily set at 1 (each sample was quantified as phosphorylated/unphosphorylated protein/tubulin). **C,** effects of U0126 in tumors 24 h post-injection in 5th week of treatment. *Left,* immunoblot analysis of phospho-ERKs, total ERK, c-Myc, phospho-c-Myc, and α-tubulin as a loading control in tumors from treated (+) and untreated (−) mice; *right,* histograms obtained as in **B**. **D,** immunoblot analyses of phospho-ERKs and ERKs in normal tissue from the same treated (+) and untreated (−) mice as in **B** (4th week). Representative immunoblot analyses. Fold increase over the control, arbitrarily set at 1, obtained by densitometric analysis. **B** to **D,** two representative control mice (*C*).

Published OnlineFirst March 3, 2009; DOI: 10.1158/1535-7163.MCT-08-0570

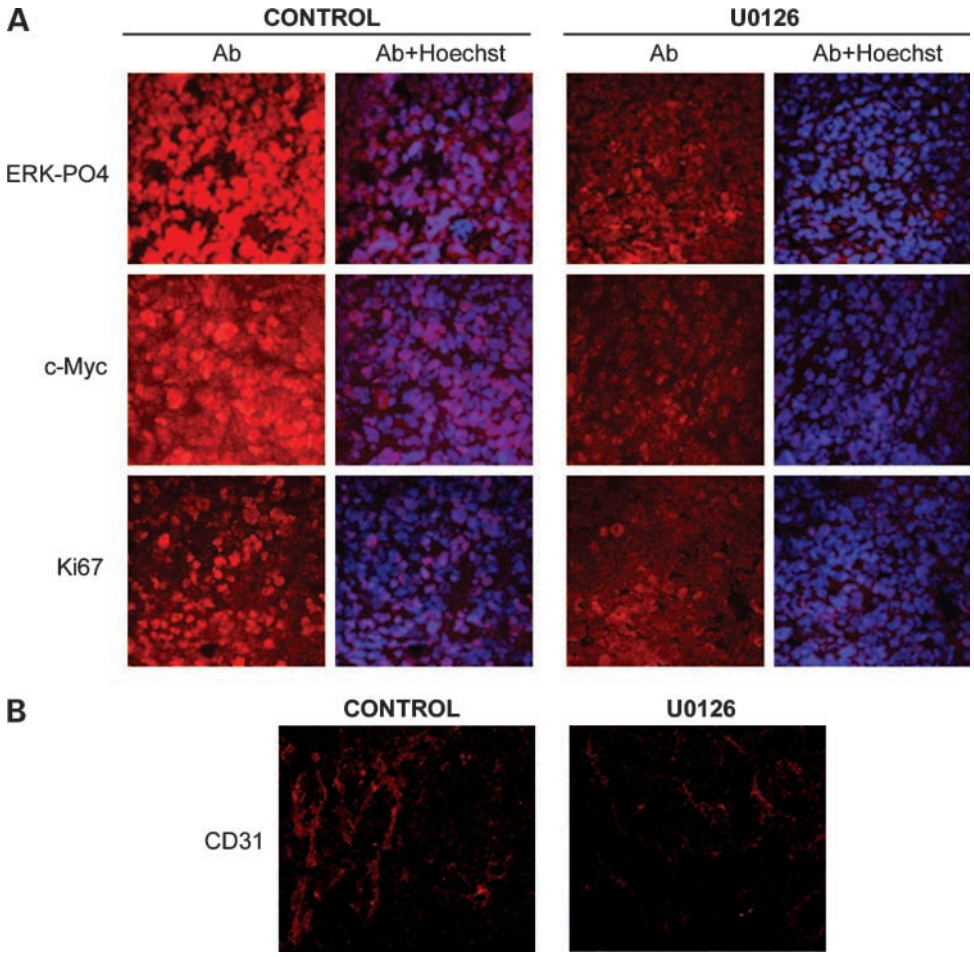

Figure 4. Morphologic analysis of the effects of U0126 treatment on phospho-ERK, c-Myc, Ki-67, and CD31 expression in tumors. **A,** immunofluorescence staining of phospho-ERKs, c-Myc, and Ki-67 (*Ab*) of cryosections. In merged images (*Ab + Hoechst*), blue nuclei are negative, whereas violet nuclei are positive for each antigen. **B,** immunofluorescence staining of CD31 shows microvessel density. Magnification, ×400 (**A**) and ×200 (**B**).

control mice yielded various highly fluorescent vascular areas, whereas tumors from treated mice were both smaller and less fluorescent (Fig. 4B).

Xenograft RD-Derived Cell Line (RD-M1) Maintains Responsiveness to U0126

We derived a more aggressive cell line after a passage in nude mice. To this end, the tumor from untreated RD-xenotransplanted mice was removed and the new cell line (RD-M1) isolated as described (Materials and Methods). The aggressiveness of RD-M1 was then tested in *in vivo* experiments. RD-M1 cells (1×10^7 per mouse) were xenotransplanted in nude mice and tumor growth was analyzed. The results showed that RD-M1 cells are more tumorigenic than parental RD cell lines as indicated by the earlier appearance of the tumor (4 versus 11 weeks; Fig. 5A). This finding suggests that RD-M1 cells acquired an aggressive potential greater than RD parental cells, although the tumor doubling time remained substantially unchanged (Fig. 5A). The ability of U0126 to block RD-M1 anchorage-independent growth was also investigated in soft agar assay. Although U0126 completely abrogated colony formation (Fig. 5A), numerous large colonies grew in vehicle-treated dishes. We thus decided to test the responsiveness of RD-M1 cells to U0126 by treating cells and studying the antigrowth biological effects of U0126 in a time course experiment and by FACS analysis. Results showed that U0126 dramatically inhibited the proliferation rate of RD-M1 (Fig. 5B). FACS analysis showed the antigrowth effect of U0126 in RD-M1, being 90% of cells arrested in the G_1 phase after 1 day of treatment (Fig. 5B). The growth-inhibitory effect of U0126 was also shown by the inhibition of CDK2 and cyclins D1, E1, and E2 (Fig. 5C). Figure 5C also shows that treatment with 10 μmol/L U0126 effectively reduced ERK and c-Myc phosphorylation, with a concomitant c-Myc level reduction as early as 6 h after treatment. As observed in the parental RD cell line (38), U0126 treatment also induced sarcomeric MHC expression in RD-M1 cells (Fig. 5C), a feature of skeletal muscle and RMS cells tending toward myogenic differentiation. Our results thus suggest that responsiveness to U0126 persisted in the more tumorigenic xenografted-derived RD-M1 cell line, suggesting that MEK inhibition may offer a new means of developing novel anticancer strategies for ERMS types.

Responsiveness of TE671 ERMS Cell Line to U0126

We used the cell line TE671 (39, 40) to explore whether the antigrowth and differentiative responses to MEK/ERK inhibition are common properties of ERMS cell lines. We

Published OnlineFirst March 3, 2009; DOI: 10.1158/1535-7163.MCT-08-0570

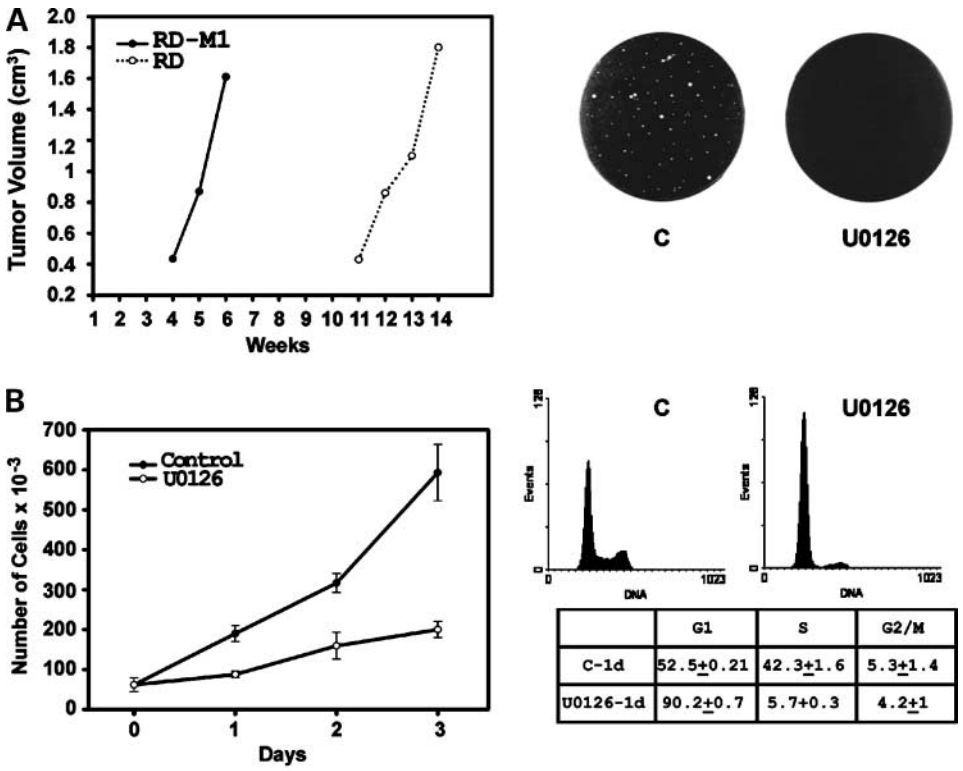

Figure 5. *In vivo* and *in vitro* growth potential of RD-M1 line derived from xenograft. **A,** schematic representation (*left*) of tumor growth delay in weeks of xenografted RD-M1 (●—●) and RD cell line (○—○). Values of RD curve are derived from Fig. 2. Soft agar assay of RD-M1 (*right*) in the absence (control) and presence of U0126. **B,** growth curve of cultured RD-M1 (*left*) in the presence (○—○) and absence (●—●) of 10 μmol/L U0126; FACS analysis (*right*) of untreated and 1-d treated RD-M1. Mean ± SE of triplicates of a representative experiment. **C,** immunoblot analyses of c-Myc, phospho-c-Myc, phospho-ERKs and total ERK, CDK2, cyclins D1, E1, and E2, and sarcomeric MHC after 6 h (*left*) and 4 d (*right*); α-tubulin as loading control. Immunoblot of MHC is not present (*left*) because sarcomeric myosin is not induced at very early treatment.

first assessed the dependence of both c-Myc phosphorylation and protein expression on ERK activity by treating TE671 with 10 μmol/L U0126. Phospho-active ERKs were strongly and persistently inhibited with a rapid (3 h) decrease in phospho-Myc and c-Myc protein levels. The decreases in phospho-Myc and c-Myc protein levels persist for 1 day of treatment (Fig. 6A), although they are detectable even after prolonged treatments (Supplementary Fig. S4).[4]

The antigrowth effect of U0126 was shown by a rapid and drastic arrest in G_1 of TE671 treated for 16 h (overnight) and 1 day as shown by FACS analysis in Fig. 6B. Anchorage-independent growth was also dramatically decreased by U0126 as shown by lack of growth in soft agar (Fig. 6C). Cell cycle arrest, induced by U0126, was corroborated by increased WAF1/p21 levels as well as by decreased cyclin D1 accumulation (Fig. 6D). As reported previously in RD cells (27), chronic U0126 treatment induced early (overnight) myogenin up-regulation and subsequent (1-3 days) MHC accumulation in TE671 (Fig. 6D). These results suggest that responsiveness to U0126 is a feature of the ERMS cell line.

Discussion

MEK/ERK pathway and c-Myc overexpression has not yet been studied in ERMS tumors. In a recent study, we showed the pivotal role of c-Myc in sustaining the transformed phenotype of an ERMS cell line (RD; ref. 27). Based on these data, we decided to investigate the effect of MEK/ERK targeting and c-Myc level on an *in vivo* RD tumor model.

Published OnlineFirst March 3, 2009; DOI: 10.1158/1535-7163.MCT-08-0570

c-Myc protein was expressed at a level higher than N-Myc protein in RD cells. The RD cell line was xenotransplanted using the highest cellular concentration (1×10^7 cells per mouse) to achieve maximum tumor uptake (100%) and large tumors to reproduce the unfavorable conditions required to effectively test an antitumor drug.

Our results show that the growth of xenotransplanted tumors is significantly reduced (48%) by U0126 treatment correlating with inhibition of phospho/active-ERK, phospho-c-Myc, and total c-Myc levels. Thus, c-Myc accumulation is via MEK/ERK.

The concomitance of phospho-ERK and c-Myc down-regulation together with a reduced tumor growth under U0126 action suggest two possible scenario: (*a*) MEK/ERK inhibition or c-Myc reduction play distinct roles in arresting growth of ERMS tumor and (*b*) a MEK/ERK/Myc axis is disrupted impairing growth of ERMS tumor.

The fact that tumor xenografts are highly responsive to U0126, whereas normal murine tissues such as lung, liver, and brain are not further suggests that ERK inhibition in nontumor cells does not persist for a long time as we have observed previously in normal cell lines *in vitro* (27). The unresponsive nature of normal tissues to the MEK inhibitor would thus lend itself to combined therapies, including this drug, as there would not be undesired side effects. Indeed, a major finding in this study is that U0126 significantly reduced tumor growth without causing intolerable toxicity as shown by 100% survival of treated mice.

Furthermore, the MEK inhibitor reduced phospho-ERK, phospho-c-Myc, and total c-Myc levels as effectively after 4 weeks of treatment as after 5 weeks, which points to the drug's effectiveness for the entire therapeutic time window. Moreover, the immunohistochemical analysis showed that whereas cells in untreated tumors were highly positive to phospho-ERK and c-Myc, particularly at a nuclear level, the number of positive cells in U0126-treated tumors was drastically reduced to an extent comparable with that observed in biochemical analyses. That U0126 effectively affects tumor growth is further supported by the drastic reduction in nuclear immunostaining for Ki-67, a typical proliferation marker that is considered to be an even more accurate indicator of MEK inhibitor-mediated decreases in melanoma tumor growth than phospho-ERK levels (41).

Herein, U0126 reduced the expression of endothelial markers such as CD31. As U0126 inhibited both ERK and c-Myc, it is not yet possible to ascribe the reduced angiogenesis to inhibition of either c-Myc or ERK pathways or both. Both c-Myc and Ras/MEK/ERK pathways have been implicated in angiogenic processes in tumors (42–44).

We provide evidence that the more tumorigenic xenograft RD-M1 cell line effectively responds to the antigrowth and differentiative action of U0126 by down-regulating

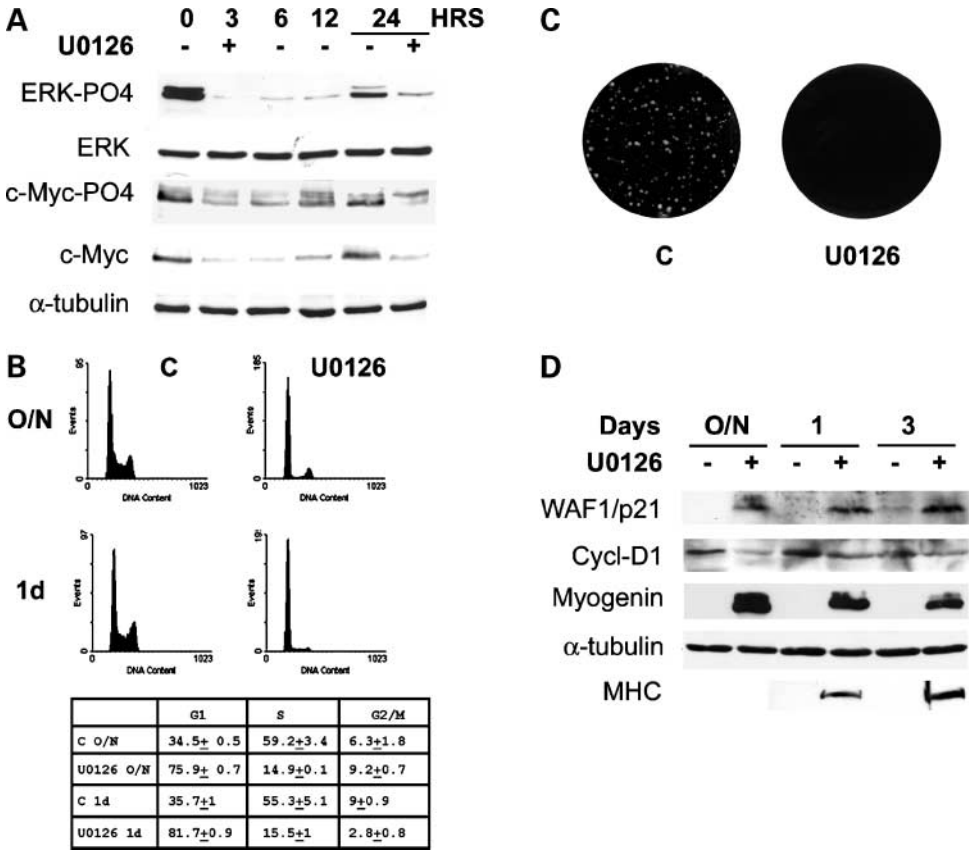

	G1	S	G2/M
C O/N	34.5± 0.5	59.2±3.4	6.3±1.8
U0126 O/N	75.9± 0.7	14.9±0.1	9.2±0.7
C 1d	35.7±1	55.3±5.1	9±0.9
U0126 1d	81.7±0.9	15.5±1	2.8±0.8

Figure 6. Effects of U0126 treatment in TE671 ERMS cell line. **A,** immunoblot analyses of phospho-ERK, total ERK, phospho-c-Myc, and c-Myc; α-tubulin as loading control. **B,** FACS analysis of untreated (*C*) overnight (16 h) and 1-d U0126-treated TE671. Mean ± SE of triplicates of a representative experiment. **C,** soft agar assay of TE671 in the absence (*C*) and presence of U0126. **D,** immunoblot analysis of WAF1/p21, cyclin D1, myogenin, and α-tubulin as loading control in untreated (−), overnight, 1- and 3-d U0126-treated cells (+). Immunoblot of MHC was done at 1 and 3 d in a different filter. Immunoblots are representative of three independent experiments; soft agar assay and FACS analysis are representative of two independent experiments.

Published OnlineFirst March 3, 2009; DOI: 10.1158/1535-7163.MCT-08-0570

both c-Myc and phospho-Myc and reducing cyclins E2 and D1. Lastly, another ERMS line, TE671, recovers growth arrest and anchorage-dependent growth under U0126 treatment, which in turn down-regulates phospho-ERK and phospho-Myc and c-Myc protein expression. The fact that U0126-mediated growth arrest in TE671 is rapidly followed by WAF1/p21 up-regulation, cyclin D1 down-regulation, and myogenic-specific marker accumulation (myogenin and MHC) further suggests that the MEK/ERK pathway and c-Myc accumulation are closely involved in maintaining malignant ERMS phenotype; indeed, their concomitant disruption leads to normal differentiated myogenic phenotype expression. Moreover, previous findings showing that cyclins, particularly cyclin D1, are down-regulated by the MEK inhibitor, in concomitance with the up-regulation of WAF1/p21 and the decrease in transformation potential, lend further support to the abnormal role of cyclins in maintaining aberrant growth of tumor cells (45, 46). Altogether, these data show that the persisting response to the antigrowth effects of MEK/ERK inhibition associated with c-Myc down-regulation is a predisposition of ERMS cells and is not overcome by altered cell aggressiveness.

The results presented here and those of our previous report indicate that the main mechanism of action of U0126 in *in vitro* and *in vivo* ERMS models is to arrest growth. This is consistent with a cytostatic mechanism that, in *in vivo* tumors, might be responsible for reduced tumor growth. The cytostatic effect of U0126 and other MEK inhibitors has been proposed previously for other tumor models (13).

In conclusion, taken together, these results suggest that MEK inhibitors are compounds that may be used in a signal transduction-based therapy for ERMS and warrant testing in preclinical and clinical ERMS trials.

Disclosure of Potential Conflicts of Interest

No potential conflicts of interest were disclosed.

Acknowledgments

We thank Dr A. Floridi for generous help and support throughout this work, R. Calabrese for useful help, F. Padula for FACS analysis, Lewis Baker for reviewing the English in the article, and ''Cassa Edile di Roma e Provincia'' for supporting part of our work.

References

1. Merlino G, Helman LJ. Rhabdomyosarcoma—working out the pathways. Oncogene 1999;18:5340–8.

2. Anderson J, Gordon A, McManus A, Shipley J, Pritchard-Jones K. Disruption of imprinted genes at chromosome region 11p15.5 in paediatric rhabdomyosarcoma. Neoplasia 1999;1:340–8.

3. Barr FG. Gene fusions involving PAX and FOX family members in alveolar rhabdomyosarcoma. Oncogene 2001;20:5736–46.

4. Keleti J, Quezado MM, Abaza MM, Raffeld M, Tsokos M. The MDM2 oncoprotein is overexpressed in rhabdomyosarcoma cell lines and stabilizes wild-type p53 protein. Am J Pathol 1996;149:143–51.

5. Germani A, Fusco C, Martinotti S, Musaro A, Molinaro M, Zani BM. TPA-induced differentiation of human rhabdomyosarcoma cells involves dephosphorylation and nuclear accumulation of mutant P53. Biochem Biophys Res Commun 1994;202:17–24.

6. Chardin P, Yeramian P, Madaule P, Tavitian A. N-ras gene activation in the RD human rhabdomyosarcoma cell line. Int J Cancer 1985;35:647–52.

7. Stratton MR, Fisher C, Gusterson BA, Cooper CS. Detection of point mutations in N-ras and K-ras genes of human embryonal rhabdomyosarcomas using oligonucleotide probes and the polymerase chain reaction. Cancer Res 1989;49:6324–7.

8. Tsumura H, Yoshida T, Saito H, Imanaka-Yoshida K, Suzuki N. Cooperation of oncogenic K-ras and p53 deficiency in pleiomorphic rhabdomyosarcoma development in adult mice. Oncogene 2006;25:7673–9.

9. Murphy LO, Blenis J. MAPK signal specificity: the right place at the right time. Trends Biochem Sci 2006;31:268–75.

10. O'Neill E, Kolch W. Conferring specificity on the ubiquitous Raf/MEK signalling pathway. Br J Cancer 2004;90:283–8.

11. Wellbrock C, Karasarides M, Marais R. The RAF proteins take centre stage. Nat Rev Mol Cell Biol 2004;5:875–85.

12. Bassel-Duby R, Olson EN. Signaling pathways in skeletal muscle remodeling. Annu Rev Biochem 2006;75:19–37.

13. Kohno M, Pouyssegur J. Pharmacological inhibitors of the ERK signaling pathway: application as anticancer drugs. Prog Cell Cycle Res 2003;5:219–24.

14. Faivre S, Djelloul S, Raymond E. New paradigms in anticancer therapy: targeting multiple signaling pathways with kinase inhibitors. Semin Oncol 2006;33:407–20.

15. Liu D, Liu Z, Condouris S, Xing M. BRAF V600E maintains proliferation, transformation, and tumorigenicity of BRAF-mutant papillary thyroid cancer cells. J Clin Endocrinol Metab 2007;92:2264–71.

16. Solit DB, Garraway LA, Pratilas CA, et al. BRAF mutation predicts sensitivity to MEK inhibition. Nature 2006;439:358–62.

17. Favata MF, Horiuchi KY, Manos EJ, et al. Identification of a novel inhibitor of mitogen-activated protein kinase kinase. J Biol Chem 1998;273:18623–32.

18. Sears R, Nuckolls F, Haura E, Taya Y, Tamai K, Nevins JR. Multiple Ras-dependent phosphorylation pathways regulate Myc protein stability. Genes Dev 2000;14:2501–14.

19. Yeh E, Cunningham M, Arnold H, et al. A signalling pathway controlling c-Myc degradation that impacts oncogenic transformation of human cells. Nat Cell Biol 2004;6:308–18.

20. Bachireddy P, Bendapudi PK, Felsher DW. Getting at MYC through RAS. Clin Cancer Res 2005;11:4278–81.

21. Adhikary S, Eilers M. Transcriptional regulation and transformation by Myc proteins. Nat Rev Mol Cell Biol 2005;6:635–45.

22. Blackwood EM, Eisenman RN. Max: a helix-loop-helix zipper protein that forms a sequence-specific DNA-binding complex with Myc. Science 1991;251:1211–7.

23. Shachaf CM, Kopelman AM, Arvanitis C, et al. MYC inactivation uncovers pluripotent differentiation and tumour dormancy in hepatocellular cancer. Nature 2004;431:1112–7.

24. Jain M, Arvanitis C, Chu K, et al. Sustained loss of a neoplastic phenotype by brief inactivation of MYC. Science 2002;297:102–4.

25. Vita M, Henriksson M. The Myc oncoprotein as a therapeutic target for human cancer. Semin Cancer Biol 2006;16:318–30.

26. Dias P, Kumar P, Marsden HB, Gattamaneni HR, Heighway J, Kumar S. N-myc gene is amplified in alveolar rhabdomyosarcomas (RMS) but not in embryonal RMS. Int J Cancer 1990;45:593–6.

27. Marampon F, Ciccarelli C, Zani BM. Down-regulation of c-Myc following MEK/ERK inhibition halts the expression of malignant phenotype in rhabdomyosarcoma and in non muscle-derived human tumors. Mol Cancer 2006;5:31.

28. Cappabianca L, Farina AR, Tacconelli A, Mantovani R, Gulino A, Mackay AR. Reconstitution of TIMP-2 expression in SH-SY5Y neuroblastoma cells by 5-azacytidine is mediated transcriptionally by NF-Y through an inverted CCAAT site. Exp Cell Res 2003;286:209–18.

29. Ciccarelli C, Marampon F, Scoglio A, et al. p21WAF1 expression induced by MEK/ERK pathway activation or inhibition correlates with growth arrest, myogenic differentiation and onco-phenotype reversal in rhabdomyosarcoma cells. Mol Cancer 2005;4:41.

30. Ju X, Katiyar S, Wang C, et al. Akt1 governs breast cancer progression *in vivo*. Proc Natl Acad Sci U S A 2007;104:7438–43.

31. Marampon F, Casimiro MC, Fu M, et al. Nerve growth factor regulation of cyclin D1 in PC12 cells through a p21RAS extracellular signal-regulated kinase pathway requires cooperative interactions between Sp1 and nuclear factor-κB. Mol Biol Cell 2008;19:2566 – 78.

32. Lowry OH, Rosebrough NJ, Farr AL, Randall RJ. Protein measurement with the Folin phenol reagent. J Biol Chem 1951;193:265 – 75.

33. Pelosi M, Marampon F, Zani BM, et al. ROCK2 and its alternatively spliced isoform ROCK2m positively control the maturation of the myogenic program. Mol Cell Biol 2007;27:6163 – 76.

34. Lee RJ, Albanese C, Fu M, et al. Cyclin D1 is required for transformation by activated Neu and is induced through an E2F-dependent signaling pathway. Mol Cell Biol 2000;20:672 – 83.

35. Wu K, Katiyar S, Li A, et al. Dachshund inhibits oncogene-induced breast cancer cellular migration and invasion through suppression of interleukin-8. Proc Natl Acad Sci U S A 2008;105:6924 – 9.

36. Horiuchi H, Kawamata H, Fujimori T, Kuroda Y. A MEK inhibitor (U0126) prolongs survival in nude mice bearing human gallbladder cancer cells with K-ras mutation: analysis in a novel orthotopic inoculation model. Int J Oncol 2003;23:957 – 63.

37. Horiuchi H, Kawamata H, Furihata T, et al. A MEK inhibitor (U0126) markedly inhibits direct liver invasion of orthotopically inoculated human gallbladder cancer cells in nude mice. J Exp Clin Cancer Res 2004;23:599 – 606.

38. Mauro A, Ciccarelli C, De Cesaris P, et al. PKCα-mediated ERK, JNK and p38 activation regulates the myogenic program in human rhabdomyosarcoma cells. J Cell Sci 2002;115:3587 – 99.

39. McAllister RM, Isaacs H, Rongey R, et al. Establishment of a human medulloblastoma cell line. Int J Cancer 1977;20:206 – 12.

40. Stratton MR, Darling J, Pilkington GJ, Lantos PL, Reeves BR, Cooper CS. Characterization of the human cell line TE671. Carcinogenesis 1989;10:899 – 905.

41. Smalley KS, Contractor R, Haass NK, et al. Ki67 expression levels are a better marker of reduced melanoma growth following MEK inhibitor treatment than phospho-ERK levels. Br J Cancer 2007;96:445 – 9.

42. Knies-Bamforth UE, Fox SB, Poulsom R, Evan GI, Harris AL. c-Myc interacts with hypoxia to induce angiogenesis *in vivo* by a vascular endothelial growth factor-dependent mechanism. Cancer Res 2004;64:6563 – 70.

43. Mavria G, Vercoulen Y, Yeo M, et al. ERK-MAPK signaling opposes Rho-kinase to promote endothelial cell survival and sprouting during angiogenesis. Cancer Cell 2006;9:33 – 44.

44. Watnick RS, Cheng YN, Rangarajan A, Ince TA, Weinberg RA. Ras modulates Myc activity to repress thrombospondin-1 expression and increase tumor angiogenesis. Cancer Cell 2003;3:219 – 31.

45. Fu M, Wang C, Li Z, Sakamaki T, Pestell RG. Minireview. Cyclin D1: normal and abnormal functions. Endocrinology 2004;145:5439 – 47.

46. Diehl JA. Cycling to cancer with cyclin D1. Cancer Biol Ther 2002;1:226 – 31.

AACR American Association for Cancer Research

Molecular Cancer Therapeutics

MEK/ERK inhibitor U0126 affects *in vitro* and *in vivo* growth of embryonal rhabdomyosarcoma

Francesco Marampon, Gianluca Bossi, Carmela Ciccarelli, et al.

Mol Cancer Ther 2009;8:543-551. Published OnlineFirst March 3, 2009.